PERIÓDICO TCHÊ QUÍMICA
ARTIGO ORIGINAL

SOLUÇÃO ANALÍTICA APROXIMADA DO PROBLEMA DE TRANSFERÊNCIA CONJUGADA DE CALOR ENTRE A CAMADA DE LIMITE E A TIRA ANISOTRÓPICA

APPROXIMATE ANALYTICAL SOLUTION OF THE PROBLEM OF CONJUGATE HEAT TRANSFER BETWEEN THE BOUNDARY LAYER AND THE ANISOTROPIC STRIP

ПРИБЛИЖЕННО-АНАЛИТИЧЕСКОЕ РЕШЕНИЕ ЗАДАЧИ О СОПРЯЖЕННОМ ТЕПЛОПЕРЕНОСЕ МЕЖДУ ПОГРАНИЧНЫМ СЛОЕМ И АНИЗОТРОПНОЙ ПОЛОСОЙ

FORMALEV, Vladimir F. [1*]; KOLESNIK, Sergey A. [2]; KUZNETSOVA, Ekaterina L. [3];

[1,2,3] Moscow Aviation Institute (National Research University), Institute No. 9 "General Engineering", 4 Volokolamskoe shosse, zip code 125993, Moscow – Russian Federation

** Correspondence author*
e-mail: formalev38@yandex.ru

Received 12 May 2019; received in revised form 14 June 2019; accepted 25 June 2019

RESUMO

A otimização de processos tecnológicos em metalurgia relacionada à transferência e uso de energia térmica cria exigências mais complicadas para o cálculo da troca de calor. Portanto, o trabalho, o método analítico aproximado para resolver os problemas conjugados da camada limite dinâmica gasosa viscosa e da condutividade térmica na faixa anisotrópica, foi desenvolvido. O artigo usou métodos numéricos modernos para resolver equações diferenciais em métodos analíticos e derivativos parciais com base em uma transformação integral de Fourier e Laplace. Equações de limite foram resolvidas analiticamente com certas simplificações, e o problema da condução de calor anisotrópico foi resolvido analiticamente. Os fluxos de calor foram determinados analiticamente pela variável longitudinal no limite da interface. Foi estabelecido que o aumento da temperatura da superfície externa contribui para que todos os fatores que impactam diretamente na magnitude dos fluxos de calor atuem em direção à sua redução. A solução analítica para o problema da condutividade térmica na faixa anisotrópica com um tipo geral de anisotropia quando o calor flui da camada limite é determinada nos limites é obtida. A pesquisa conduzida para a temperatura do limite externo e fluxo de calor do gás para ele demonstra que com o aumento do grau de anisotropia longitudinal a temperatura superficial da tira a jusante aumenta a partir do aumento da condução longitudinal de calor Um método de conjugação original usando os fluxos contínuos de calor e temperaturas no limite da interface foi encontrado. Os resultados numéricos para os fluxos de calor e temperaturas no limite da interface foram obtidos e analisados.

Palavras-chave: *tensor de condutividade térmica, transferência de calor acoplada, distribuição de temperatura, distribuição de fluxos de calor, principais componentes do tensor de condutividade térmica*.

ABSTRACT

Optimization of technological processes in metallurgy related to transfer and use of heat energy makes more complicated demands for calculation of heat exchange. Therefore, the work, the approximate analytical method for solving the conjugate problems of viscous gas-dynamic boundary layer and thermal conductivity in the anisotropic strip, has been developed. The paper uses modern numerical methods for solving differential equations in partial derivative and analytic methods on the basis of an integral transform of Fourier and Laplace. Boundary equations have been solved analytically with certain simplifications, and the problem of anisotropic heat conduction has been solved analytically. The heat flows are determined analytically by the longitudinal variable at the interface boundary. It has been established that temperature increase of the external surface contributes to that all factors directly impacting on the magnitude of heat flows act towards their reduction. The analytical solution for the problem of thermal conductivity in the anisotropic strip with a general type of anisotropy when the heat flows from the boundary layer are determined at the boundaries is obtained. The conducted research for the temperature of external boundary and heat flow from gas to it demonstrates that with increasing the degree of longitudinal anisotropy the surface temperature of the strip downstream increases from increasing longitudinal heat conduction An original conjugation method using the continuous heat flows, and temperatures at the interface boundary is found. The numerical results for the heat flows and temperatures at

DOI: 10.52571/PTQ.v16.n32.2019.590_Periodico32_pgs_572_582.pdf

the interface boundary have been obtained and analyzed.

Keywords: *thermal conductivity tensor, coupled heat transfer, temperature distribution, distribution of heat flows, main components of thermal conductivity tensor*.

АННОТАЦИЯ

Оптимизация технологических процессов в металлургии, связанных с переносом и использованием тепловой энергии, представляет все более сложные требования к расчету теплообмена. Поэтому в работе разработан приближенно-аналитический метод решения сопряженных задач вязкого газодинамического пограничного слоя и теплопроводности в анизотропной полосе. В работе используются современные численные методы решения дифференциальных уравнений в частных производных, а также аналитические методы на основе интегральных преобразований Фурье и Лапласа. Уравнения пограничного слоя решены аналитически с некоторыми упрощениями, а задача анизотропной теплопроводности решена аналитически. На границе сопряжения аналитически определяются распределения по продольной переменной тепловые потоки. Установлено, что увеличение температуры наружной поверхности способствует тому, что все факторы, которые имеют непосредственное влияние на величину тепловых потоков, действуют в сторону их уменьшения. Получено аналитическое решение задачи теплопроводности в анизотропной полосе с анизотропией общего вида, когда на границах определяются тепловые потоки от пограничного слоя. Проведенное исследование для температуры наружной границы и тепловых потоков к ней от газа показывают, что при увеличении степени продольной анизоторопии температура поверхности полосы вниз по потоку увеличивается с увеличения продольного компонента теплопроводности. Найден оригинальный метод сопряжения с использованием непрерывных тепловых потоков и температур на границе сопряжения. Получены и проанализированы численные результаты по тепловым потокам и температурам на границе сопряжения.

Ключевые слова: *тензор теплопроводности, сопряженный теплообмен, распределения температур, распределение тепловых потоков, главные компоненты тензора теплопроводности*.

---

1. INTRODUCTION

When solving the problems of the aero and gas-dynamic heating of high-speed aircrafts the following partial problems shall be solved:

- determination of heat flows from the high-temperature viscous gas-dynamic flows to the external surfaces of aircrafts;

- determination of non-stationary temperature fields in the structural elements of aircrafts under the impact of heat flows from the gas;

- docking (conjugation) at the “gas – body” boundary of heat flows and temperatures from gas with heat flows and temperatures in the body.

Traditionally, the heat flows from gas to the body, and then the problems of the theory of thermal conductivity in a body with boundary conditions in the form of these heat flows were formed and solved separately which led to the errors in temperatures of up to 50%. The joint solution of these two problems faces the difficulties associated with the following features: the physics of heat transfer in the gas and in the body are described by the various partial differential equations; the type of these equations is different; the viscous gas dynamics equations are most often stationary, and the equations of thermal conductivity are non-stationary (Skvortsov *et al.*, 2000; Dmitriev *et al.*, 2011; Amirgaliyev *et al.*, 2017). In addition, if the streamlined bodies are anisotropic, then the difficulties associated with anisotropy are added, namely: tensor nature of thermal conductivity as a result of which the thermal conductivity equations contain the mixed derivatives; setting and solving only the multidimensional non-stationary problems; the boundary conditions of the second kind contain all the components of the temperature gradient (Kazanin et al., 2019; Korshunov et al., 2016).

With respect to the anisotropic theory of thermal conductivity, including in the composite materials, it is possible to distinguish the works (Formalev, 2001; Formalev and Kolesnik, 2007; Formalev *et al.*, 2009; Formalev and Kolesnik, 2013; Formalev *et al.*, 2016a; Formalev *et al.*, 2016b; Formalev *et al.*, 2017a; Formalev *et al.*, 2017b; Formalev *et al.*, 2018a). With respect to the coupled problems of the boundary layer and thermal conductivity, including the anisotropic one, one can cite works (Formalev *et al.*, 2015a;

Kolesnik *et al.*, 2015; Formalev *et al.*, 2015b; Formalev and Kolesnik, 2016; Prokofiev *et al.*, 2016;Formalev *et al.*, 2016c; Okonechnikov *et al.*, 2016; Formalev and Kolesnik, 2018; Formalev and Kolesnik, 2017b; Lurie *et al.*, 2017; Babaytsev *et al.*, 2017; Gidaspov and Severina, 2017 Formalev and Kolesnik, 2017a; Formalev *et al.*, 2018c; Bulychev *et al.*, 2018a; Rabinskiy *et al.*, 2018; Bulychev *et al.*, 2018b; Bulychev *et al.*, 2018c; Bulychev *et al.*, 2018d; Gidaspov *et al.*, 2018; Formalev *et al.*, 2018b;). This paper states and solves for the first time in the approximate analytical manner the problem of conjugate (joint) heat transfer between the boundary layer and the thermal conductivity in the anisotropic strip.

2. MATERIALS AND METHODS

When formulating the complex problem of the conjugate heat transfer between the boundary layer and the anisotropic strip, the following assumptions are made:

- in the equations of conservation of momentum and energy for the boundary layer the inertial forces are small compared to the forces of friction and pressure;

- heat transfer in the boundary layer is quasi-stationary, i.e., stationary at each time point;

- heat transfer in the body is non-stationary;

- the velocity vector of the incoming flow is perpendicular to the axis Ox (Figure 1).

In accordance with these assumptions, the system of equations for the problem of conjugate heat transfer will be as follows as in Equations 1 – 17.

To solve the general problem (Equation 1 – Equation 17), it is possible to use the analytical solution of the problem of anisotropic thermal conductivity (Equation 8 – Equation 17) for which a constant value of the heat flow density $\lambda\frac{\partial T}{\partial y}\Big|_{y=0} \eta(l-|x|)=q_w,\ x\in(-l,+l)$ in the conjugation condition (Equation 9) is set at the beginning. Such a solution was for the first time obtained by the authors through the consistent application of the Fourier transform with respect to variable x and the Laplace transform with respect to a variable t. It has the following form Equations 18 – 24, herewith (Equations 25, 26), here $\delta(\tau-0)-$ is the Dirac delta function.

3. RESULTS AND DISCUSSION:

To determine q_w in Equation 18 let us integrate by variable y the momentum conservation Equation 1 using the boundary conditions (Equation 4) and (Equation 6), we obtain (Equation 27) using which in the energy Equation 2 we will find the temperature distribution Equations 28 – 31 differentiating which by y at border $y=0$ we will get Equation 32.

Equation 32 cannot be substituted into Equation 18 since in Equation 18 q_w is constantly on an interval $x\in(-l,+l)$, and the values q_w calculated by Equation 32 change significantly along with the variable x. Therefore, to reconcile (32) with Equation 18, the following procedure is used (Figure 2).

The interval $x\in(0,\,l)$ by points $x_i,\ i=\overline{1,\,n}$ is divided into n elementary areas $\Delta x_i=x_{i+1}-x_i$ where the value of the heat flow density is assumed to be constant and equal to $q_{w_i}=(q_w(x_{i+1})+q_w(x_i))/2,\ i=\overline{1,\,n}$. Similarly, taking into account the symmetry q_w with respect to point $x=0$, the interval $x\in(-l,\,0)$ is divided (Figure 2a). As a result, the elementary heat flow density q_{wi} at the intervals $(-x_{i+1},-x_i)$ and (x_i,x_{i+1}) is equal to the difference between the densities of the heat flows acting at the intervals $(-x_{i+1},x_{i+1})$ and $(-x_i,x_i)$ (Figure 2b), i.e. $q_{wi}=q_{wi}\eta(x_{i+1}-|x|)-q_{wi}\eta(x_i-|x|)$, and the entire heat flow Equation 19 from the boundary layer to the boundary *w* is equal to the sum (Equation 33). This approach allows to obtain an Equation 18 and use the principle of superposition for each term of Equation 33. Then the temperature of interface boundary *w* can be found from the solution of the system of transcendental equations obtained by the superposition of solutions (18) for each combined Equation 33 (Equation 34).

The system of nonlinear Equations 34 with respect to $T_w(x_0),\,T_w(x_1),...,T_w(x_{n-1})$ is solved using the Newton method. Using $T_w(x_j),\ j=\overline{0,n-1}$ it is possible to determine the density of heat flows Equation 33 substituting,

which in Equation 18, we will obtain the temperature distribution in the plate.

Figures 3, 4 shows the results for calculations of the conjugate heat transfer based on the analytical Equation 18 and Equation 33. Figure 3 shows the temperature $T_w(x)$ of the boundary w, both for the isotropic case (curve 1) and for the orthotropic case (curves 2, 3), and Figure 4 shows the values of the heat flow density at the boundary w depending on the longitudinal coordinate x and the degree of anisotropy $(\lambda_\xi / \lambda_\eta)$.

The original data adopted the following values:

$u_e(x) = 2000x,\ m/s; \quad T_e(x) = 2210 - 200x,\ K;$

$l = 0.09m; \quad l_1 = 0.005; \quad l_T = 0,01m;$

$\lambda_\eta = 0.02kW/m \cdot K; \quad \lambda_\xi / \lambda_\eta = 1,10,100,$

$c\rho = 2500\frac{kJ}{m^3 K},\ \varphi = 0,\ q_{w1} = 0.$

Since the orthotropic strip is considered, the off-diagonal components of the thermal conductivity tensor in relations (Equation 15) are equal to zero $\lambda_{12} = \lambda_{21} = 0,$, and the orientation angle φ of the main axes $O\xi,\ O\eta,$ of the thermal conductivity tensor is equal to zero; herewith, the diagonal components $\lambda_{11} > 0$ and $\lambda_{22} > 0$ are different. From relations (Equation 15) it can be seen that when $\varphi = 0$ $\lambda_{11} = \lambda_\xi,$ $\lambda_{22} = \lambda_\eta,$ that is, the diagonal components of the thermal conductivity tensor are equal to the principal values of the thermal conductivity tensor λ_ξ and λ_η. In this case (in case of orthotropy), the symmetry is observed in the distribution of temperatures and heat fluxes relative to the vertical axis $x = 0,$, that is, in Figures 3 and 4 $\left.\frac{\partial T}{\partial x}\right|_{x=0} = 0$ and $\left.\frac{\partial q_w}{\partial x}\right|_{x=0} = 0.$. Next, from Figure 3, it can be seen that the higher the longitudinal component of the thermal conductivity tensor $\lambda_\xi,$ is, the higher the temperature at the periphery of the strip will be. Thus, at $\lambda_\xi / \lambda_\eta = 1$ $(\lambda_\eta = 0,02kW/m \cdot K)$ the minimum temperature at $x = 0,09m$ is equal to zero, for $\lambda_\xi / \lambda_\eta = 10$ $T\max = 550K,,$ and at $\lambda_\xi / \lambda_\eta = 100$ $T\max = 1150K.$

This situation with the temperature of the external boundary of the strip creates the opposite picture for the heat flows $q_w,$ presented in Figure 4 for the same cases $\lambda_\xi = 1,10,100.$ It is clear that with an increase in temperature, the heat flows to this boundary significantly decrease due to the temperature difference between the gas and the body, as well as due to the increase in dynamic viscosity which reduces the Reynolds numbers and, consequently, the thermal ones, and also decreases the gas density which also reduces the heat flows.

Thus, with an increase in the temperature of the external surface, all the factors affecting the magnitude of the heat flow act in the direction of decreasing the latter. Thus, from Figure 4, when $\lambda_\xi / \lambda_\eta > 1$ the heat flows on the periphery of the strip adopt the negative values, that is, the strip does not heat up, but cools. This fact can be used as the thermal protection only by using a strip material with a degree of orthotropy of at least 10, i.e. $\lambda_\xi / \lambda_\eta \geq 10.$

Designations: $I -$ total enthalpy, $I = \int_0^T c_p dT + u^2/2$; $\Pr$ is Prandtl number, $\Pr = \frac{\mu c_p}{\lambda}$; $\rho, u, T, p -$ respectively, is the density, the longitudinal component of velocity vector, temperature, pressure; $\lambda, c, \mu -$ is the thermal conductivity, heat capacity, dynamic viscosity of axis $Ox, Oy -$ of the Cartesian coordinate system for the boundary layer; Ox, Oy_T are the axes of the Cartesian coordinate system for the body; $t -$ is the time; $O\xi, O\eta -$ are the principal axes of the thermal conductivity tensor; $l, l_1 -$ is the the length of the regions affected by the non-zero heat flows, respectively, on the boundaries w and w_1; l_T is the plate thickness; $\lambda_{11}, \lambda_{12}, \lambda_{21}, \lambda_{22} -$ are the components of the thermal conductivity tensor; $\lambda_\xi, \lambda_\eta -$ are the components of the thermal conductivity tensor, reduced to the main axes; $\varphi -$ is the angle between the main axis $O\xi$ and the axis Ox; $q -$ is the heat flow density; $\delta_e -$ is the boundary layer thickness; $\eta -$ is the single function. *Indices:* $e -$ the external boundary of the boundary layer; $w -$ is the gas-body interface; $w1 -$ is the internal boundary of the plate; $w2, w3 -$ are the side boundaries of the plate; $t -$ is the body.

4. CONCLUSIONS:

The article established and solved the problem of conjugate heat transfer between the thermal gas-dynamic boundary layer and the orthotropic strip; herewith, the components of the thermal conductivity tensor in the orthotropic case are equal to the main thermal conductivity coefficients. The boundary layer equations are solved analytically with some simplifications, and the anisotropic thermal conductivity problem is solved analytically. The entire adjoint problem is reduced to the integral equation (Volterra equation of the first kind). The results obtained for the temperature of the external boundary and the heat flows to it from the gas demonstrate that with increasing degree of longitudinal anisotoropia, the temperature of the strip surface downstream increases with increase in the longitudinal component of thermal conductivity. As a result, the heat flows to the surface of the strip from the boundary layer sharply decrease and even become negative, that is, the strip cools off. This phenomenon is a consequence of the decrease in the temperature gradient from the gas to the body, increase in the dynamic viscosity of the gas, and decrease in the density of the gas with an increase in the surface temperature.

There is a practical possibility of developing the thermal protection without the additional costs and structures, only using the thermal protection in contact with the high-temperature boundary layer, with a degree of longitudinal anisotropy of the order of 10.

5. ACKNOWLEDGMENTS:

This work was supported by the Russian Foundation for Basic Research grants No 18-01-00446A, No 18-01-00444A, No 17-01-00587A and the Grant of the President of the Russian Federation: МД-1250.2018.8.

6. REFERENCES:

[1] Amirgaliyev, Y., Wójcik, W., Ospanova, T., Jetpisov, K. *Journal of Ecological Engineering*, **2017**, *18*(6), 1-7

[2] Babaytsev, A.V., Prokofiev, M.V., Rabinskiy, L.N. *International Journal of Nanomechanics Science and Technology*, **2017**, *8*(4), 359-366. DOI: 10.1615/NanoSciTechnolIntJ.v8.i4.60.

[3] Bulychev, N.A., Kazaryan, M.A., Ethiraj, A., Chaikov, L.L. *Bulletin of the Lebedev Physics Institute*, **2018a**, *45*(9), 263-266.

[4] Bulychev, N.A., Kazaryan, M.A., Kirichenko, M.N., Garibyan, B.A., Morozova, E.A., Chernov, A.A. *Proc. SPIE*, **2018b**, *10614*, 1061411.

[5] Bulychev, N.A., Kazaryan, M.A., Zakharyan, A.R., Bodryshev, V.V., Kirichenko, M.N., Shevchenko, S.N., Yakunin, V.G., Timoshenko, V.Yu., Bychenko, A.B. *Proc. SPIE*, **2018c**, *10614*, 1061412.

[6] Bulychev, N.A., Kuznetsova, E.L., Bodryshev, V.V., Rabinskiy, L.N. *Nanoscience and Technology. An International Journal*, **2018d**, *9*(2), 91-97. DOI: 10.1615/NanoSciTechnolIntJ.2018025703.

[7] Dmitriev, A.I., Skvortsov, A.A., Koplak, O.V., Morgunov, R.B., Proskuryakov, I.I. *Physics of the Solid State*, **2011**, *53*(8), 1547-1553.

[8] Formalev, V.F. *Teplofizika Vysokikh Temperatur*, **2001**, *39*(5), 810.

[9] Formalev, V.F., Kolesnik, S.A. *High Temperature*, **2007**, *45*(1), 76-84.

[10] Formalev, V.F., Kolesnik, S.A. *High Temperature*, **2013**, *51*(6), 795-803.

[11] Formalev, V.F., Kolesnik, S.A. *High Temperature*, **2017a**, *55*(4), 564-569.

[12] Formalev, V.F., Kolesnik, S.A. *International Journal of Heat and Mass Transfer*, **2018**, *123*, 994-998.

[13] Formalev, V.F., Kolesnik, S.A. *Journal of Engineering Physics and Thermophysics*, **2016**, *89*(4), 975-984.

[14] Formalev, V.F., Kolesnik, S.A. *Journal of Engineering Physics and Thermophysics*, **2017b**, *90*(6), 1302-1309.

[15] Formalev, V.F., Kolesnik, S.A., Kuznetsova, E.L. *Composites: Mechanics, Computations, Applications*, **2018b**, *9*(3), 223-237.

[16] Formalev, V.F., Kolesnik, S.A., Kuznetsova, E.L. *High Temperature*, **2009**, *47*(2), 228-234.

[17] Formalev, V.F., Kolesnik, S.A., Kuznetsova, E.L. *High Temperature*, **2018a**, *56*(3), 393-397.

[18] Formalev, V.F., Kolesnik, S.A., Kuznetsova, E.L. *High Temperature*, **2017a**, *55*(5), 761-766.

[19] Formalev, V.F., Kolesnik, S.A., Kuznetsova, E.L. *High Temperature*, **2016a**, *54*(6), 824-830.

[20] Formalev, V.F., Kolesnik, S.A., Kuznetsova, E.L. *High Temperature*, **2018**, *56*(5), 727-731.

[21] Formalev, V.F., Kolesnik, S.A., Kuznetsova, E.L. *High Temperature*, **2015a**, *53*(5), 697-702.
[22] Formalev, V.F., Kolesnik, S.A., Kuznetsova, E.L. *Periodico Tche Quimica*, **2018c**, *15* (Special Issue 1), 426-432.
[23] Formalev, V.F., Kolesnik, S.A., Kuznetsova, E.L., Rabinskii, L.N. *High Temperature*, **2016b**, *54*(3), 390-396.
[24] Formalev, V.F., Kolesnik, S.A., Kuznetsova, E.L., Rabinskiy, L.N. *International Journal of Pure and Applied Mathematics*, **2016c**, *111*(2), 303-318.
[25] Formalev, V.F., Kolesnik, S.A., Selin, I.A., Kuznetsova, E.L. *High Temperature*, **2017b**, *55*(1), 101-106.
[26] Formalev, V.F., Kuznetsova, E.L., Rabinskiy, L.N. *High Temperature*, **2015b**, *53*(4), 548-553.
[27] Gidaspov, V.Y., Moskalenko, O.A., Severina, N.S. *High Temperature*, **2018**, *56*(5), 751-757.
[28] Gidaspov, V.Y., Severina, N.S. *High Temperature*, **2017**, *55*(5) 777–781.
[29] Kakhramanov, R.M., Knyazeva, A.G., Rabinskiy, L.N., Solyaev, Y.O. *High Temperature*, **2017**, *55*(5), 731-736.
[30] Kazanin, O.I., Korshunov, G.I., Rudakov, M.L. *Innovation-Based Development of the Mineral Resources Sector: Challenges and Prospects – 11th conference of the Russian-German Raw Materials*, **2019**, *2018*, 571-577.
[31] Kolesnik, S.A., Formalev, V.F., Kuznetsova, E.L. *High Temperature*, **2015**, *53*(1), 68-72.
[32] Korshunov, G.I., Rudakov, M.L., Stepanova, L.V. Pollution Research, **2016**, *35*(4), 919-922.
[33] Lurie, S.A., Rabinskiy, L.N., Polyakov, P.O., Sitnikov, S.A., Solyaev, Y.O. *International Journal of Nanomechanics Science and Technology*, **2017**, *8*(4), 347-358. DOI: 10.1615/ NanoSciTechnolIntJ.v8.i4.50.
[34] Okonechnikov, A.S., Rabinskiy, L.N., Tarlakovskii, D.V., Fedotenkov, G.V. *International Journal of Nanomechanics Science and Technology*, **2016**, *7*(1), 61-75. DOI: 10.1615/ NanomechanicsSciTechnolIntJ.v 7.i2.10.
[35] Prokofiev, M.V., Vishnevskii, G.E., Zhuravlev, S.Y., Rabinskiy, L.N. *International Journal of Nanomechanics Science and Technology*, **2016**, *7*(2), 97-105. DOI: 10.1615/ NanomechanicsSciTechnolIntJ.v 7.i1.40.
[36] Rabinskiy, L.N., Kuznetsova, E.L. *Periodico Tche Quimica*, **2018**, *15*(Special Issue 1), 339-347.
[37] Skvortsov, A.A., Orlov, A.M., Frolov, V.A., Gonchar, L.I., Litvinenko, O.V. *Physics of the Solid State*, **2000**, *42*(10), 1861-1864.

$$-\frac{\partial p}{\partial x}+\frac{\partial}{\partial y}\left(\mu(T)\frac{\partial u}{\partial y}\right)=0,\ \ 0<y<\delta_e(x),\ 0<x<l; \qquad \text{(Eq. 1)}$$

$$\frac{\partial}{\partial y}\left[\lambda(T)\frac{\partial T}{\partial y}+\frac{\mu(T)}{2}\left(1-\frac{1}{\mathrm{Pr}}\right)\frac{\partial u^2}{\partial y}\right]=0,\ \ 0<y<\delta_e(x),\ 0<x<l; \qquad \text{(Eq. 2)}$$

$$p=\rho RT,\ 0<y<\delta_e(x),\ 0<x<l; \qquad \text{(Eq. 3)}$$

$$u(x,0)=0,\ \ y=0,\ \ 0<x<l; \qquad \text{(Eq. 4)}$$

$$u(x,\delta_e(x))=u_e(x),\ T(x,\delta_e(x))=T_e(x),\ T(x,0)=T_w(x), \qquad \text{(Eq. 5)}$$

$$\frac{dp_e}{dx}=-\rho u_e\frac{du_e}{dx},\ \ y=\delta_e(x),\ 0\le x\le l; \qquad \text{(Eq. 6)}$$

$$T\big|_{y_T=0}=T\big|_{y=0}=T_w,\ -\infty<x<\infty,\ y_T=y=0,\ t>0; \qquad \text{(Eq. 7)}$$

$$c\rho\frac{\partial T}{\partial x}=\lambda_{11}\frac{\partial^2 T}{\partial x^2}+2\lambda_{12}\frac{\partial^2 T}{\partial x\partial y}+\lambda_{22}\frac{\partial^2 T}{\partial y^2},\ -\infty<x<\infty,\ 0<y<l_T,\ t>0; \qquad \text{(Eq. 8)}$$

$$-\left(\lambda_{21}\frac{\partial T}{\partial x}+\lambda_{22}\frac{\partial T}{\partial y_T}\right)\Bigg|_{y_T=0}=\lambda\frac{\partial T}{\partial y}\Bigg|_{y=0}\cdot\eta\left(l-|x|\right) \qquad \text{(Eq. 9)}$$

$$-\infty<x<\infty,\ y_T=y=0,\ t>0; \qquad \text{(Eq. 10)}$$

$$\left(\lambda_{21}\frac{\partial T}{\partial x}+\lambda_{22}\frac{\partial T}{\partial y}\right)\Bigg|_{y_T=l_T}=q_{w1}\eta\left(l_1-|x|\right),\ -\infty<x<\infty,\ y_T=l_T,\ t>0; \qquad \text{(Eq. 11)}$$

$$\eta(\psi)=\begin{cases}1,\ \psi>0\\ 0,\ \psi<0;\end{cases} \qquad \text{(Eq. 12)}$$

$$\lambda_{11}\frac{\partial T}{\partial x}+\lambda_{12}\frac{\partial T}{\partial y}=0,\ \ x\to-\infty,\ 0<y_T<l_T,\ t>0; \qquad \text{(Eq. 13)}$$

$$\lambda_{11}\frac{\partial T}{\partial x}+\lambda_{12}\frac{\partial T}{\partial y}=0,\ \ x\to\infty,\ 0<y_T<l_T,\ t>0\ ; \qquad \text{(Eq. 14)}$$

$$\begin{aligned}&\lambda_{11}=\lambda_\xi\cos^2\varphi+\lambda_\eta\sin^2\varphi,\\ &\lambda_{22}=\lambda_\xi\sin^2\varphi+\lambda_\eta\cos^2\varphi,\\ &\lambda_{12}=\lambda_{21}=\left(\lambda_\xi-\lambda_\eta\right)\sin\varphi\cos\varphi;\end{aligned} \qquad \text{(Eq. 15)}$$

$$T(x,y_T,0)=0,\ -\infty<x<\infty,\ 0<y_T<l_T,\ t=0; \qquad \text{(Eq. 16)}$$

$$\frac{\partial T}{\partial x}=\frac{\partial T}{\partial y}=0,\ x\to\pm\infty,0<y_T<l_T,\ t\geq 0\,. \qquad \text{(Eq. 17)}$$

$$T(x,y,t)=\frac{q_w}{2\lambda_{22}\gamma l_T}\int_0^t F_1(x,y,\tau)\Theta_3^-(y,\tau)d\tau+\frac{q_{w1}}{2\lambda_{22}\gamma l_T}\int_0^t F_2(x,y,\tau)\Theta_3^+(y,\tau)d\tau \qquad \text{(Eq. 18)}$$

$$F_1(x,y,\tau)=\operatorname{erf}\frac{\sqrt{\gamma}(l+\alpha y-x)}{2\sqrt{\beta\tau}}+\operatorname{erf}\frac{\sqrt{\gamma}(l-\alpha y+x)}{2\sqrt{\beta\tau}}, \qquad \text{(Eq. 19)}$$

$$F_2(x,y,\tau)=\operatorname{erf}\frac{\sqrt{\gamma}\left(l_1+\alpha(y-l_T)-x\right)}{2\sqrt{\beta\tau}}+\operatorname{erf}\frac{\sqrt{\gamma}\left(l_1-\alpha(y-l_T)+x\right)}{2\sqrt{\beta\tau}}\,, \qquad \text{(Eq. 20)}$$

$$\Theta_3^-(y,\tau)=1+2\sum_{k=1}^{\infty}\cos\frac{k\pi y}{l_T}\exp\left(-\frac{k^2\pi^2}{\gamma l_T^2}\tau\right), \qquad \text{(Eq. 21)}$$

$$\Theta_3^+(y,\tau)=1+2\sum_{k=1}^{\infty}\cos\frac{k\pi(l_T-y)}{l_T}\exp\left(-\frac{k^2\pi^2}{\gamma l_T^2}\tau\right), \qquad \text{(Eq. 22)}$$

$$\alpha=\lambda_{12}/\lambda_{22},\ \beta=\lambda_\xi\lambda_\eta/\lambda_{22}^2,\ \gamma=c\rho/\lambda_{22}, \qquad \text{(Eq. 23)}$$

$$\operatorname{erf}(z)=\frac{2}{\sqrt{\pi}}\int_0^z\exp\left(-\xi^2\right)d\xi\,. \qquad \text{(Eq. 24)}$$

$$\frac{\partial\Theta_3^-(y,\tau)}{\partial y}=\begin{cases}-\dfrac{2\pi}{l_T}\displaystyle\sum_{k=1}^{\infty}k\sin\frac{k\pi y}{l_T}\exp\left(-\frac{k^2\pi^2}{\gamma l_T^2}\tau\right), & 0<y<l_T\\ \gamma l_T\delta(\tau)\equiv\gamma l_T\delta(\tau-0), & y=0\\ 0, & y=l_T,\end{cases} \qquad \text{(Eq. 25)}$$

$$\frac{\partial\Theta_3^-(y,\tau)}{\partial y}=\begin{cases}\dfrac{2\pi}{l_T}\displaystyle\sum_{k=1}^{\infty}k\sin\frac{k\pi(l_T-y)}{l_T}\exp\left(-\frac{k^2\pi^2}{\gamma l_T^2}\tau\right), & 0<y<l_T\\ 0, & y=0\\ \gamma l_T\delta(\tau)\equiv\gamma l_T\delta(\tau-0), & y=l_T.\end{cases} \qquad \text{(Eq. 26)}$$

$$u(x,y)=\frac{1}{2\mu_w}\frac{dp_e(x)}{dx}\left(y^2-\delta_e(x)y\right)+u_e(x)\frac{y}{\delta_e(x)}, \qquad \text{(Eq. 27)}$$

$$T(x,y)=T_w(x)-\frac{k\mu_w}{\lambda_w}\left(\frac{\alpha_1}{4}y^4+\frac{\beta_1}{3}y^3+\frac{\gamma_1}{2}y^2\right)+$$
$$\left[\frac{T_e(x)-T_w(x)}{\delta_e(x)}+\frac{k\mu_w}{\lambda_w}\left(\frac{\alpha_1}{4}\delta_e^3(x)+\frac{\beta_1}{3}\delta_e^2(x)+\frac{\gamma_1}{2}\delta_e(x)\right)\right]y, \quad \text{(Eq. 28)}$$

$$k=1-\frac{1}{\mathrm{Pr}},\quad \alpha_1=\frac{1}{2\mu_w^2}\left(\frac{dp_e}{dx}\right)^2, \quad \text{(Eq. 29)}$$

$$\beta_1=-\frac{3}{4}\frac{\delta_e(x)}{\mu_w^2}\left(\frac{dp_e}{dx}\right)^2+\frac{3u_e(x)}{2\mu_w\delta_e(x)}\left(\frac{dp_e}{dx}\right), \quad \text{(Eq. 30)}$$

$$\gamma_1=\left(\frac{\delta_e(x)}{2\mu_w}\frac{dp_e}{dx}\right)^2-\frac{u_e(x)}{\mu_w}\frac{dp_e}{dx}+\frac{u_e^2(x)}{\delta_e^2(x)}. \quad \text{(Eq. 31)}$$

$$q_w=\lambda_w\left.\frac{\partial T}{\partial y}\right|_{y=0}=\lambda_w\frac{T_e(x)-T_w(x)}{\delta_e(x)}+k\mu_w\left[\frac{\alpha}{4}\delta_e^3(x)+\frac{\beta}{3}\delta_e^2(x)+\frac{\gamma}{2}\delta_e(x)\right] \quad \text{(Eq. 32)}$$

$$q_w=\sum_{i=0}^{n-1}\left[q_{wi}\eta(x_{i+1}-|x|)-q_{wi}\eta(x_i-|x|)\right]. \quad \text{(Eq. 33)}$$

$$T_w(x_j)\approx\sum_{i=0}^{n-1}\left\{q_w(x_i,T_w(x_i))\eta(x_{i+1}-|x|)\frac{1}{\lambda_{22}\gamma\ l_T}\int_0^t F_1(x_j,0,\tau,x_{i+1})\Theta_3^-(0,\tau)d\tau-\right.$$
$$\left.-q_w(x_i,T_w(x_i))\eta(x_i-|x|)\frac{1}{\lambda_{22}\gamma\ l_T}\int_0^t F_1(x_j,0,\tau,x_i)\Theta_3^-(0,\tau)d\tau\right\}+ \quad \text{(Eq. 34)}$$
$$+\frac{q_{w1}}{\lambda_{22}\gamma\, l_T}\int_0^t F_2(x_j,l_T,\tau)\Theta_3^+(l_T,\tau)d\tau,\quad j=\overline{0,n-1}.$$

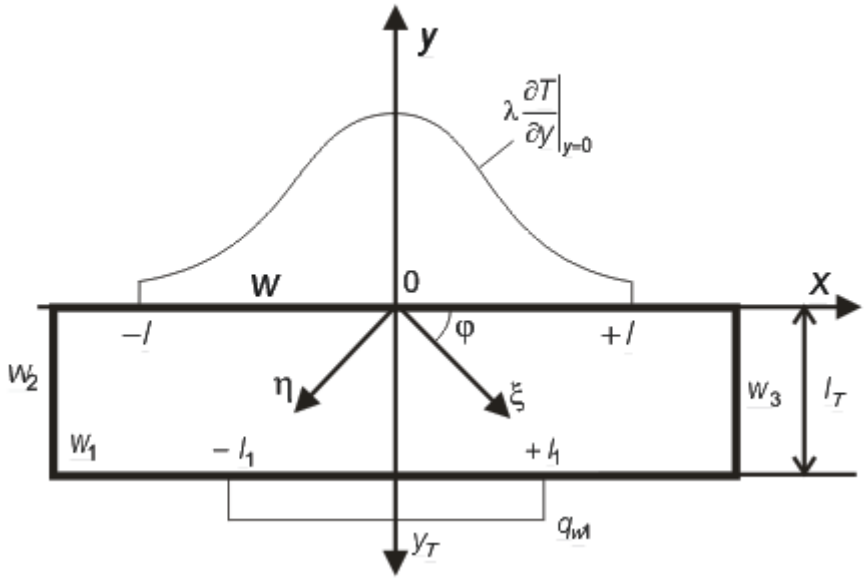

Figure 1. *Design diagram*

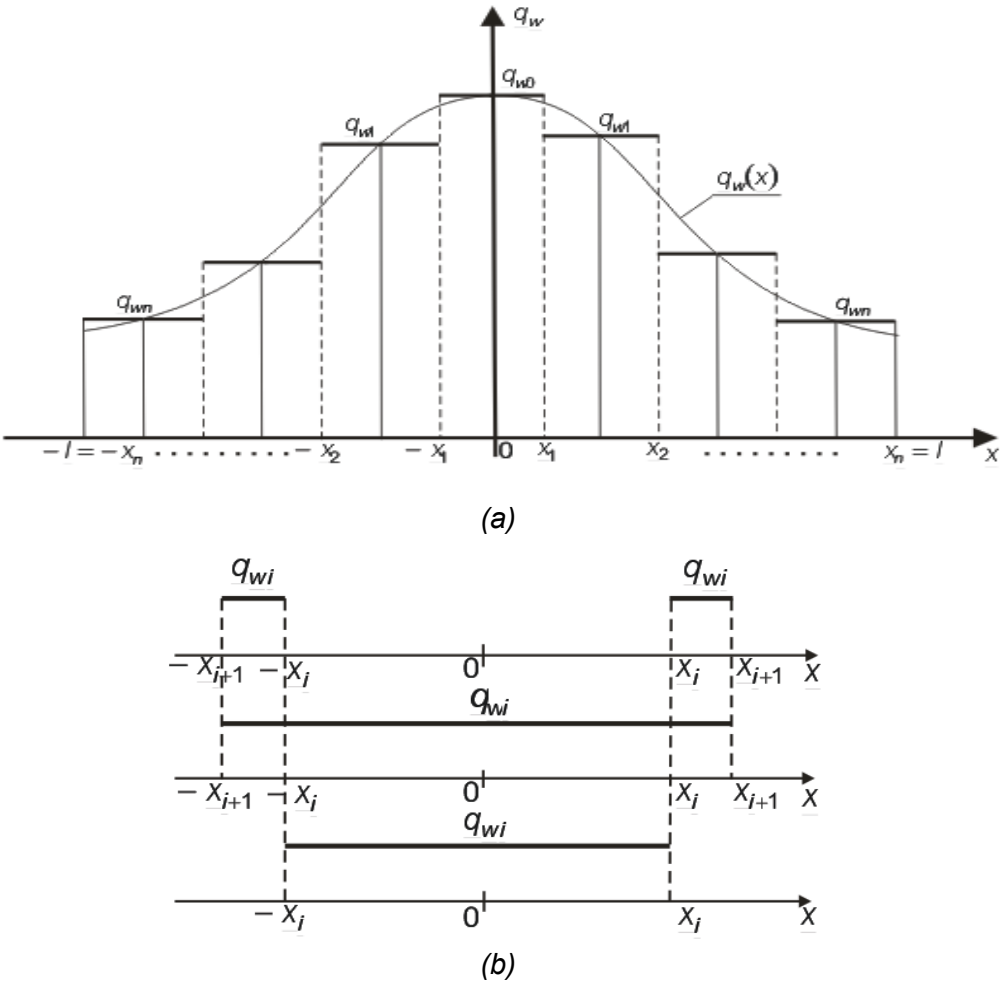

Figure 2. *Splitting the interface boundary into the areas with constant values of the heat flows density: (a) partitioning method; (b) overlay method*

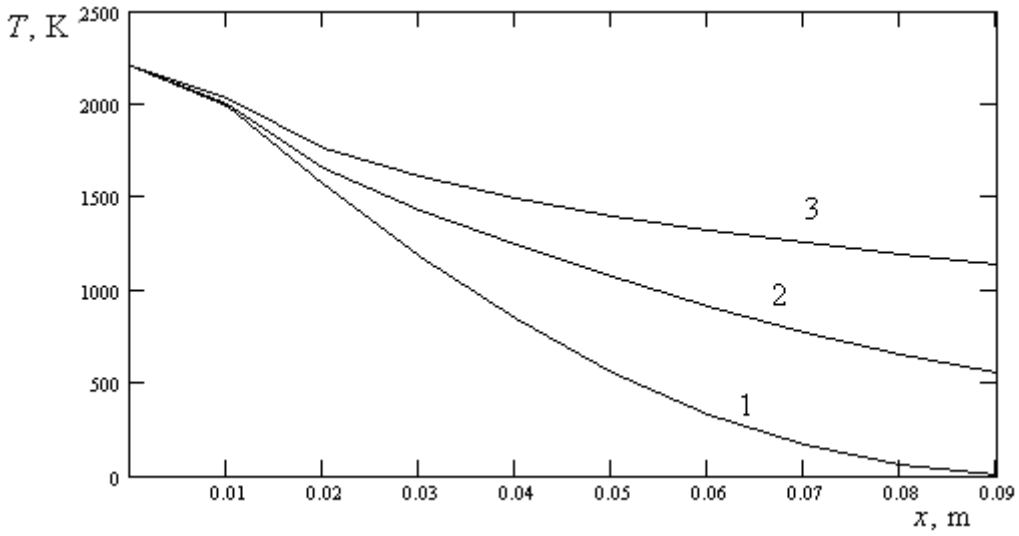

Figure 3. *Comparison of the temperature distribution at the interface boundary for the isotropic and orthotropic cases* $\left(\lambda_\eta = 0,02kW/m\cdot K\right)$*:*

1– $\lambda_\xi / \lambda_\eta = 1$*; 2–* 10*; 3–* 100*.*

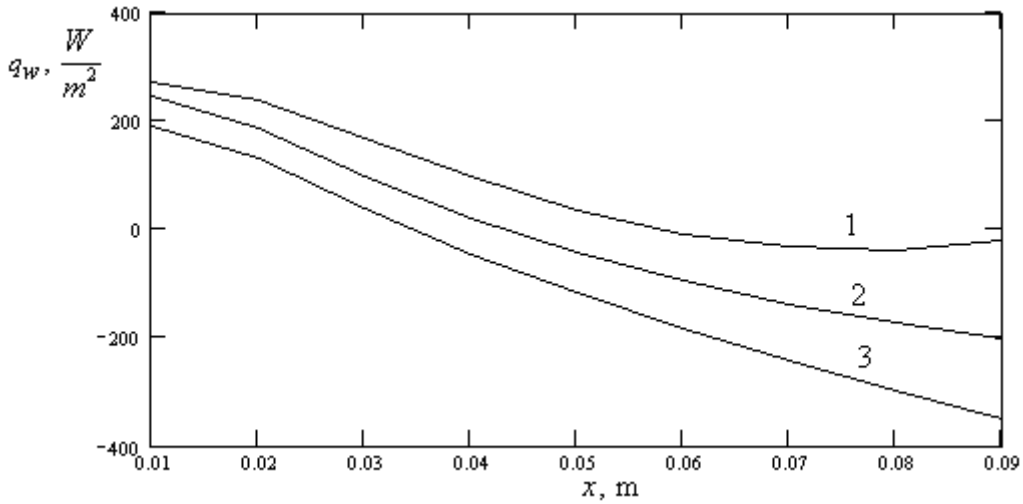

Figure 4. *Comparison of the distribution of the density of heat flows from the boundary layer at the interface boundary for the isotropic and orthotropic cases* $\left(\lambda_\eta = 0,02kW/mK\right)$*:*

1 – $\lambda_\xi / \lambda_\eta = 1$*; 2 –* 10*; 3–*100*.*